Thermochimica Acta, 78 (1984) 285–295
Elsevier Science Publishers B.V., Amsterdam – Printed in The Netherlands

KINETICS OF THE THERMAL DECOMPOSITION OF ALUMINUM SULFATE

KAN-SEN CHOU and CHYUAN-SHIUH SOONG

Department of Chemical Engineering, National Tsing Hua University, Hsinchu, Taiwan (R.O.C.)

(Received 19 March 1984)

ABSTRACT

The kinetics of the thermal decomposition of aluminum sulfate has been studied both isothermally and dynamically in a Perkin-Elmer thermobalance. The contracting-volume model is found to be the best one for describing the kinetic results under isothermal conditions. The general phase boundary reaction models, including 1-D, 2-D and 3-D, are then used to analyze the data from dynamic measurements. Under various conditions, such as different heating rates and sample weights, the most appropriate kinetic expression changes from the 3-D phase boundary reaction model at slow heating rates and small sample weights to the 1-D model at the other extremes. The distribution of thermal flux, in terms of the external heat transport effect, is thought to be the predominant factor here. Finally, a linear compensation effect is also observed between the calculated apparent activation energies and pre-exponential factors from the dynamic studies.

INTRODUCTION

Though complex in nature, the kinetics of the thermal decomposition of solid-state materials has been studied quite extensively due to its practical importance. In this type of study, the rate of change of the fraction of material decomposed, α, with respect to time is often expressed as follows

$$\frac{\mathrm{d}\alpha}{\mathrm{d}t} = k\mathrm{f}(\alpha) \tag{1}$$

where $\mathrm{f}(\alpha)$ depends upon the characteristic reaction mechanism and k is the rate constant which has an Arrhenius-type relationship with temperature.

$$k = Z\exp(-E_\mathrm{a}/RT) \tag{2}$$

However, due to the difficulty in obtaining accurate differential data from strip charts, the integrated form of eqn. (1) is used here instead.

$$\mathrm{g}(\alpha) = \int_0^\alpha \frac{\mathrm{d}(\alpha)}{\mathrm{f}(\alpha)} = \int_0^t k\,\mathrm{d}t \tag{3}$$

Under isothermal conditions where the rate constant k is independent of

0040-6031/84/$03.00

reaction time, a plot of g(α) vs. time should then give a straight line if the correct form of g(α) is used. In Table 1, the set of kinetic equations examined in this study is listed. Their derivations can easily be found in the literature [1–3].

With dynamic techniques, the temperature of the system is usually set to increase at a constant rate, q, i.e.

$$\mathrm{d}T = q\mathrm{d}t \tag{4}$$

Then, by combining eqns. (2), (3) and (4), we obtain

$$\mathrm{g}(\alpha) = \frac{Z}{q}\int_0^T \exp(-E_\mathrm{a}/RT)\mathrm{d}T = \frac{ZE_\mathrm{a}}{Rq}\mathrm{p}(x) \tag{5}$$

where the function of p(x) is defined as

$$\mathrm{p}(x) = \frac{\mathrm{e}^{-x}}{x} - \int_x^\infty \frac{\mathrm{e}^{-u}}{u}\mathrm{d}u \tag{6}$$

where $u = E_\mathrm{a}/RT$ and x is the corresponding value of u at which a fraction α of material has decomposed.

Several approaches have been proposed to calculate E_a and Z values from experimental data using eqn. (5) [4–6]. For its simplicity and accuracy, the Zsako method is used here [7]. In this method, eqn. (5) is rewritten in its logarithmic form as follows

$$\log\frac{ZE_\mathrm{a}}{Rq} = \log \mathrm{g}(\alpha) - \log \mathrm{p}(x) = B \tag{7}$$

Theoretically, B should depend upon the nature of the compound studied and upon the heating rate, but not upon the temperature, and, hence, it is a constant for each run. Therefore, for each kinetic equation tested, a trial-and-error procedure is used to find the optimum E_a value which gives the maximum constancy of B. This constancy is quantitatively characterized by

TABLE 1

List of kinetic equations examined in this work

Symbol	g(α)	Model
R_1	α	One-dimensional phase boundary reaction
R_2	$1-(1-\alpha)^{1/2}$	Two-dimensional phase boundary reaction
R_3	$1-(1-\alpha)^{1/3}$	Three-dimensional phase boundary reaction
D_1	α^2	One-dimensional diffusion
D_2	$\alpha+(1-\alpha)\ln(1-\alpha)$	Two-dimensional diffusion
D_3	$[1-(1-\alpha)^{1/3}]^2$	Jander equation
D_4	$(1-\frac{2}{3}\alpha)-(1-\alpha)^{2/3}$	Ginstling–Brounshtein equation
F_1	$-\ln(1-\alpha)$	First-order kinetics
A_2	$[-\ln(1-\alpha)]^{1/2}$	Random nucleation; Avrami equation
A_3	$[-\ln(1-\alpha)]^{1/3}$	Random nucleation; Erofeev equation

the standard deviation, δ, of individual B_i values from their arithmetic mean of $\overline{B}$. And δ is defined as

$$\delta = \left[\frac{\sum_{i=1}^{r} \left(B_i - \overline{B}\right)^2}{r} \right]^{1/2} \tag{8}$$

where r is the number of data points from each TG curve used for the calculation of B_i and $\overline{B}$. In the present work, data were taken at α values varying from 0.05 to 0.95 at an equal interval of 0.05 to give a total of 19 points.

By comparison of the minimum δ values calculated for each kinetic equation, $g(\alpha)$, one would then be able to determine the most appropriate reaction mechanism for the compound being investigated. The corresponding pre-exponential factor will then be found from the following equation

$$\log Z = \overline{B} + \log Rq - \log E_a \tag{9}$$

The kinetics of the decomposition reaction of aluminum sulfate to give alumina powders with high reactivity and high sinterability has been studied by a number of researchers [8–11]. Yet only the isothermal technique was used in most of these works. Papazian et al. [10] tried the dynamic method, but reported that no variation in apparent activation energy was found with heating rate. This conclusion was clearly in contrast with that observed for calcium carbonate by Gallagher and Johnson [12,13]. It is therefore the objective of this study to investigate in more detail the kinetics of the decomposition of aluminum sulfate using both isothermal and dynamic techniques.

EXPERIMENTAL

For both the isothermal and dynamic measurements, a Perkin-Elmer TGS-2 thermobalance was used. This unit was calibrated periodically with magnetic standards to ensure consistency. Weight changes vs. temperature were recorded on strip charts. Reagent grade aluminum sulfate hydrate ($Al_2(SO_4)_3 \cdot 16–18\ H_2O$, Osaka Hayashi Co.) was used as the starting material. Powders weighed from about 2 to 30 mg and were loosely packed in a platinum crucible of 5.8 mm diameter and 1.8 mm depth. These samples were first dehydrated by heating to 450 °C and then calcined at constant heating rates for dynamic studies until the completion of the decomposition reaction. For a few runs at the 20 °C min^{-1} heating rate, the experiments were stopped before the samples reached constant weights due to the temperature limit (1000 °C) of the equipment. As for the isothermal runs, the temperatures were raised at 160° min^{-1} to the appropriate values after

TABLE 2

Comparison of the fit of various kinetic equations to the isothermal results

Symbols	850 °C	870 °C	880 °C	890 °C	900 °C	910 °C	920 °C
R_1	0.967	0.968	0.955	0.946	0.972	0.966	0.967
R_2	0.995	0.996	0.991	0.986	0.998	0.966	0.995
R_3 [a]	0.999	1.000	0.998	0.997	1.000	0.999	0.999
D_1	0.998	0.997	0.996	0.988	0.997	0.997	0.998
D_2	0.995	0.994	0.993	0.996	0.993	0.995	0.995
D_3	0.963	0.965	0.974	0.982	0.960	0.967	0.963
D_4	0.988	0.988	0.994	0.995	0.985	0.989	0.988
F_1	0.990	0.992	0.994	0.992	0.990	0.993	0.990
A_2	0.988	0.991	0.983	0.981	0.993	0.990	0.988
A_3	0.972	0.976	0.963	0.960	0.979	0.974	0.972

[a] The best fitting model based on these results.

the dehydration step. Dry air flowing at 15 ml min^{-1} was used throughout this study. The effects of sample weight and heating rate on the decomposition kinetics of anhydrous aluminum sulfate were investigated.

RESULTS AND DISCUSSION

Isothermal measurements

Though the dynamic studies can theoretically yield more information on a single measurement, the isothermal studies are still used very often as

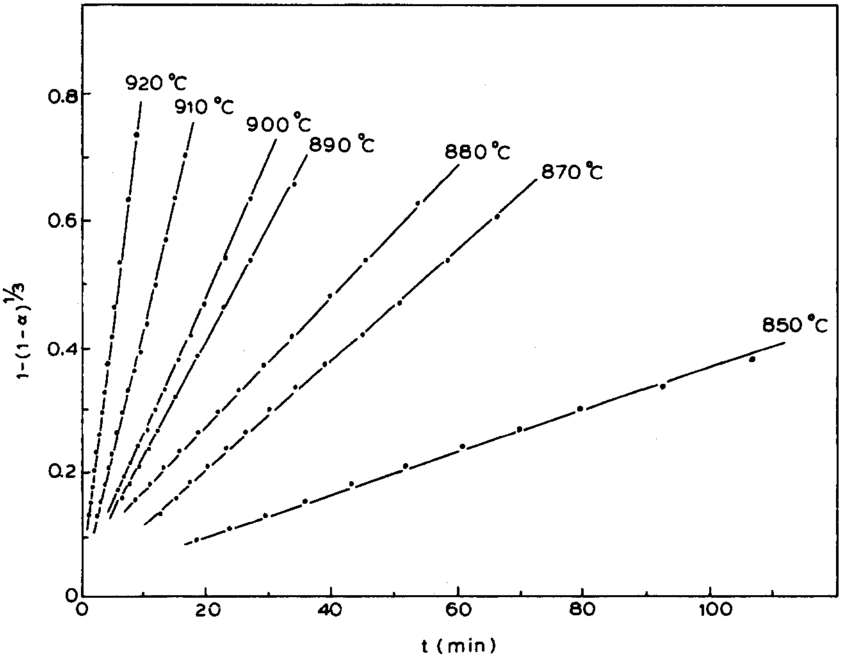

Fig. 1. Isothermal decomposition data according to the contracting volume model.

references. Small sample weights of 5–6 mg were used here. The reaction temperature varied from 850 to 920 °C. Data of conversion vs. time were analyzed according to eqn. (3) by the reduced time method [1,3] to determine the most appropriate kinetic equation for describing this decomposition reaction. As can be seen from Table 2, the contracting volume model (i.e., the three-dimensional phase boundary reaction model) gives the highest correlation coefficients at all temperatures. Based on this model, plots of $1-(1-\alpha)^{1/3}$ vs. time are shown in Fig. 1. Rate constants at different temperatures were then calculated and fitted to the Arrhenius equation (Fig. 2) to give an apparent activation energy of $E_a = 115$ kcal mol^{-1} and pre-exponential factor, $Z = 4.71 \times 10^{18}$ s^{-1}.

Our conclusion on the best fitting kinetic model is the same as that reported in the literature. However, the value of the calculated activation energy is higher than 64 kcal mol^{-1} reported by Warner and Ingraham [8], 74 kcal mol^{-1} by Johnson and Gallagher [9] and 95.3 kcal mol^{-1} by

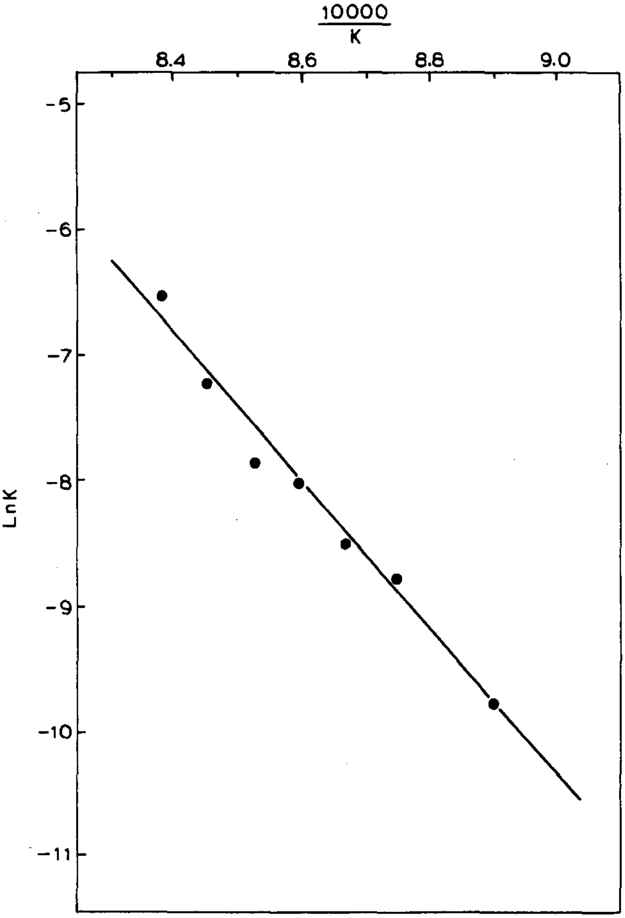

Fig. 2. Arrhenius plot of rate constants calculated from isothermal results.

Papazian et al. [10]. However, a difference of this magnitude in activation energy is not uncommon in this type of study. The variations in equipment design and the starting material can have significant effects on the observed E_a values.

Dynamic measurements

In view of the conclusion from isothermal studies, only the phase boundary reaction models (R_1, R_2 and R_3 in Table 1) were used to analyze the dynamic results. Generally, the movement of the reactant–product interface in a decomposition reaction is controlled by heat and mass transfer, rather than by the chemical or bond-breaking steps [12–14]. The heat from the furnace is first transported to the surface of a decomposing particle or pellet by conduction and radiation through the atmosphere and the sample holder. It is then transported by conduction from the surface through the product layer to the reaction interface. At the same time, the gaseous product has to diffuse outwardly from the interface and be carried away in the sweep gas. Under various operating conditions, the relative resistance of each of the

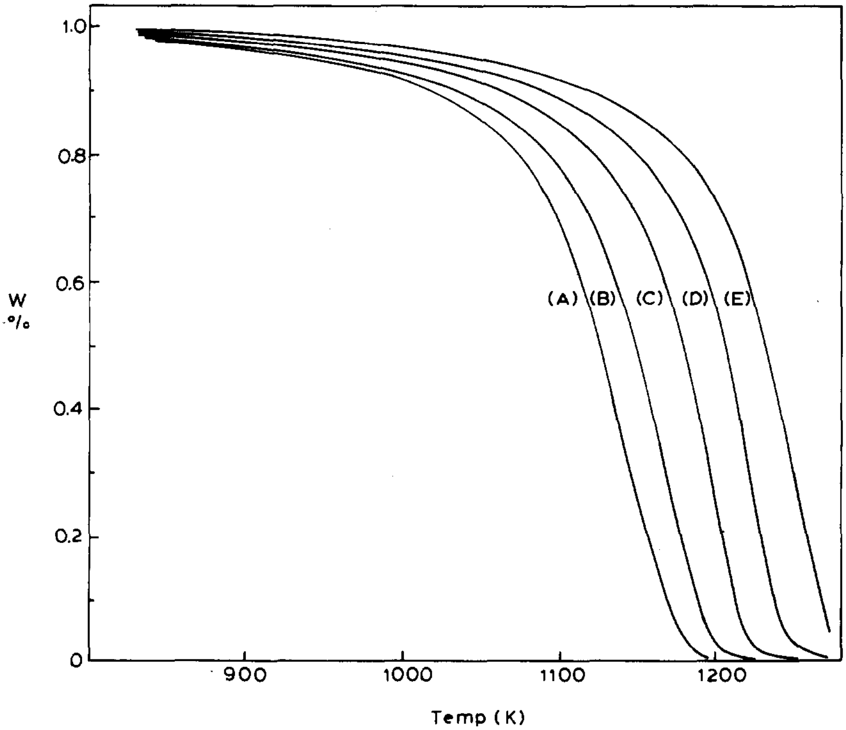

Fig. 3. Representative weight changes from dynamic measurements. These curves were obtained for nominal sample weights of 10.5 mg which were heated at (A) 1.25, (B) 2.5, (C) 5.0, (D) 10.0, and (E) 20.0 °C min^{-1}.

above transport steps then determines the observed reaction rate and hence the apparent kinetic parameters.

In order to single out the effect of heating rate, runs were made for nominal sample weights of 10.5 mg at different heating rates of 1.25, 2.50, 5.0, 10.0 and 20.0 °C $\min^{-1}$. The corresponding TG curves were shown in Fig. 3. Based on these data, the $\delta_{\min}$ values were then calculated according to the Zsako method and are listed in Table 3 for the three phase boundary reaction models. As can be seen here, the most appropriate kinetic model, judged by the $\delta_{\min}$ values, changes from the three-dimensional model for slow heating rates at 1.25 and 2.50 °C $\min^{-1}$, to the two-dimensional model at 5.0 °C $\min^{-1}$ and finally to the one-dimensional model at fast heating rates of 10.0 and 20.0 °C $\min^{-1}$. The kinetic parameters E_a and Z were, therefore, determined in accordance with the respective kinetic model for each heating rate which are also listed in Table 3 for comparison purposes.

In general, the calculated apparent activation energies and pre-exponential factors increase as the heating rate decreases. By drawing smooth curves through these data (Fig. 4), we can extrapolate to the zero heating rate to get values which are in good agreement with the isothermal results of 115 kcal mol^{-1} and 4.71×10^{18} s^{-1}.

Since in the apparatus used in the present work, the measuring thermocouple was about 1 cm below that of the sample holder, significant time lags were observed between the measured temperature and that of the sample at fast heating rates (Fig. 3). This suggests that, under these conditions, the external heat transfer step plays the most important role.

Due to the difference in thermal transport properties between the atmosphere and the sample holder, a distribution of thermal flux around the sample surface is very likely. As a result, the decomposition reaction of the sample pile will probably start from the hotter side and then move forward. This is therefore equivalent to a one-dimensional phase boundary reaction controlled process. On the other hand, when the sample pile is decomposed isothermally or heated at slow heating rates, all sides of the pile would have

TABLE 3

Effect of heating rate on the calculated minimum standard deviations and kinetic parameters for different models

Heating rate (°C $\min^{-1}$):	1.25	2.50	5.0	10.0	20.0
$\delta_{\min}(R_3)$	0.02741	0.03666	0.02951	0.07970	0.07403
$\delta_{\min}(R_2)$	0.05321	0.04524	0.01789	0.06658	0.06126
$\delta_{\min}(R_1)$	0.06742	0.06869	0.02498	0.04167	0.03390
E_a [a] kcal mol^{-1}	86	76	68	54.5	48
log Z^* s^{-1}	12.82	11.05	9.69	7.02	5.96

[a] In the calculation of E_a and Z values, model R_3 was used for 1.25 and 2.50 °C $\min^{-1}$ runs, R_2 for the 5.0 °C $\min^{-1}$ run and R_1 for the 10.0 and 20.0 °C $\min^{-1}$ runs.

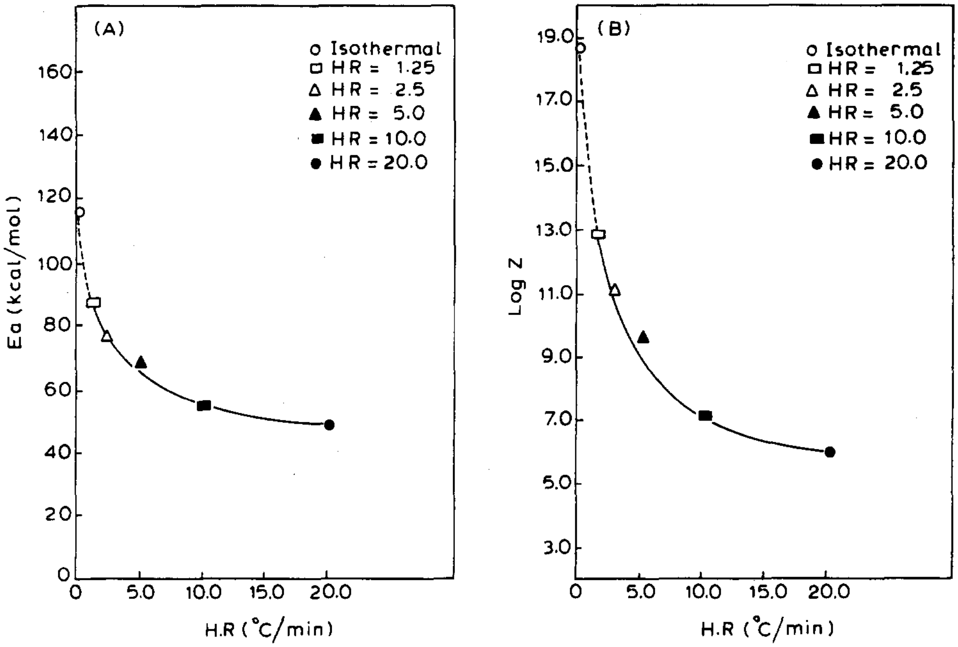

Fig. 4. Effect of heating rate on calculated kinetic parameters. (A) Apparent activation energy, and (B) pre-exponential factor.

a more or less equal temperature. This situation then corresponds to the contracting volume model. For other heating rates, a compromise, i.e., the two-dimensional model, will then become appropriate.

In the above discussion, the sample pile was tacitly assumed to behave in the same manner as a compressed pellet. This was also suggested by Kato et al. [11]. A loosely-packed sample pile differs from a pellet mainly in that it has more void space among particles. Heat transport through this space should have a positive effect on the movement of the reaction interface. Nevertheless, the diffusion of the gaseous product also uses the same space, only in the opposite direction. It might therefore cancel out, at least partly, the positive effect by heat transport and give the observed overall effect.

The effects of sample weight were studied at several heating rates and their results are listed in Table 4. Based on these data, it is obvious that in the dynamic technique the sample weight would have a smaller effect than the heating rate. Samples of various quantities will produce piles with different geometric factors, which, as suggested by Gallagher and Johnson [12], would have similar effects on the decomposition reactions as the distribution of thermal flux. This should explain qualitatively the changes from models R_3 to R_2 for the series of runs made at 5.0 °C min^{-1}. However, at higher rates, the distribution of thermal flux will have a more dominant effect as indicated by the results in Table 4. Their discussion [12] about other

TABLE 4

Effect of sample weight on the calculated kinetic parameters

Sample weight (mg)	E_a (kcal mol^{-1})	log Z (s^{-1})	Model
Heating rate = 5.0 °C min^{-1}			
1.87	85	13.30	R_3
2.25	80	12.11	R_3
5.46	77	11.25	R_2
6.58	76	11.02	R_2
10.40	68	9.69	R_2
14.20	65	9.01	R_2
Heating rate = 10.0 °C min^{-1}			
0.94	63	8.72	R_1
2.54	57	7.42	R_1
5.12	56	7.19	R_1
6.74	55	6.92	R_1
8.98	54	6.82	R_1
10.60	54	6.79	R_1
13.36	53	6.69	R_1
Heating rate = 20.0 °C min^{-1}			
1.60	50	6.06	R_1
3.70	47	5.62	R_1
5.60	45	5.17	R_1
7.00	46	5.37	R_1
10.80	48	5.96	R_1
14.80	44	4.85	R_1

potential effects of sample weights in the study of calcium carbonate, such as the self-cooling effect and the partial pressures of the product gases, should also apply well to the present work.

Finally, the compensation effect was also observed for the calculated kinetic parameters from the dynamic measurements. The linear relationship obtained from Fig. 5 is as follows

$$\log Z = 0.198E_a - 3.82 \tag{10}$$

SUMMARY AND CONCLUSION

The kinetics of the thermal decomposition of anhydrous aluminum sulfate was investigated both isothermally and dynamically. In the isothermal studies, the contracting volume model, i.e., the 3-D phase boundary reaction model, was found to best fit the measured results. An apparent activation energy of 115 kcal mol^{-1} and a pre-exponential factor of 4.71×10^{18} s^{-1}

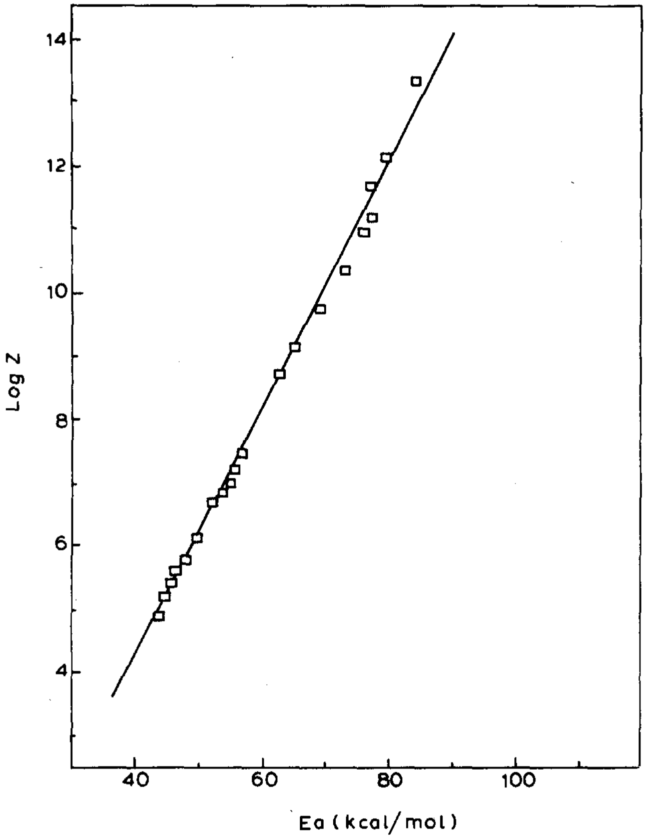

Fig. 5. The kinetic compensation effect.

were determined from the calculated rate constants.

In the dynamic measurements, the effects of heating rate and sample weight on the kinetic parameters were studied. When these data were analyzed by the Zsako method, it was found that the best fitting kinetic expression changed from the 3-D phase boundary reaction model for slow heating rates and small sample weights to the 1-D phase boundary reaction model for the other extremes. This seems to suggest that a distribution of thermal flux, caused by different thermal transport properties between the atmosphere and the sample holder, plays a very important role in determining the apparent kinetic equation and parameters.

Generally, the apparent activation energies increase as the heating rate decreases. It extrapolates to reasonably good agreement with the isothermal results, indicating consistency for the calculated parameters. The effect of sample weight is not as significant as that of the heating rate. Its decrease also caused an increase in the calculated apparent activation energies, to a lesser extent. Finally, a linear relationship, i.e., the compensation effect, was observed for log Z and E_a and it has the following form

$$\log Z = 0.198\ E_a - 3.82$$

ACKNOWLEDGMENT

The authors thank National Tsing Hua University for financial support of this research work.

REFERENCES

1 J.H. Sharp, G.W. Brindley and B.N.N. Achar, J. Am. Ceram. Soc., 49 (1966) 379.
2 S.F. Hulbert, J. Br. Ceram. Soc., 6 (1969) 11.
3 J.M. Criado, Thermochim. Acta, 24 (1978) 186.
4 C.D. Doyle, J. Appl. Polym. Sci., 5 (1961) 285.
5 H.H. Horowitz and G. Metzger, Anal. Chem., 35 (1963) 1464.
6 A.W. Coats and J.P. Redfern, Nature (London), 201 (1964) 68.
7 J. Zsako, J. Phys. Chem., 72 (1968) 2406.
8 N.W. Warner and T.R. Ingraham, Can. J. Chem. Eng., 40 (1962) 263.
9 D.W. Johnson and P.K. Gallagher, J. Am. Ceram. Soc., 54 (1971) 461.
10 H.A. Papazian, P.J. Pizzolato and R.R. Orrell, Thermochim. Acta, 4 (1972) 97.
11 E. Kato, K. Daimon and M. Nanbu, J. Am. Ceram. Soc., 64 (1981) 436.
12 P.K. Gallagher and D.W. Johnson, Thermochim. Acta, 6 (1973) 67.
13 P.K. Gallagher and D.W. Johnson, Thermochim. Acta, 14 (1976) 255.
14 A.W.D. Hills, Chem. Eng. Sci., 23 (1968) 297.